Dynamic CFD modeling of calcination in a rotary lime kiln with an external dryer

JAROD RYAN, MARKUS BUSSMANN,
AND NIKOLAI DEMARTINI

ABSTRACT: Mid-kiln ring formation is a problem in lime kilns that may be related to fluctuations in the start location of calcination. To calculate fluctuations in bed and gas temperature profiles within a lime kiln with an external dryer, a dynamic two-dimensional (2D) axisymmetric computational fluid dynamics (CFD) gas model with a methane burner implemented in ANSYS Fluent, coupled by mass and heat balances to a one-dimensional (1D) bed model, was developed. The dynamic model was used to calculate changes in the location where calcination starts with fluctuations in operational conditions using pulp mill data.

This model simulates radiative, convective, and conductive heat transfer between the gas, wall, and bed to determine the axial bed temperature in the kiln. The calcination reaction is described using a shrinking core model that allows for the prediction of the location at which calcination begins and the degree of calcination achieved. The solid motion within the kiln is modeled using Kramer's equation modified for transient response.

Steady-state and dynamic simulation results were compared to data from an industrial dry lime kiln, and good agreement was found. A sensitivity analysis was also performed to provide insight on how operating conditions and model variables impact the calcination location and degree of calcination. Of the variables examined, the fuel rate and the feed temperature had the largest impact on both the calcination location and degree of calcination in the kiln. Model predictions of a period of ring formation in the industrial kiln showed that the start location of calcination fluctuated by more than 2 m on either side of the mean of regular operation, warranting further investigation of the importance of these fluctuations on mid-kiln ring formation.

Application: The work done in this paper gives insight into the impact that different operating conditions have on the calcination start location. It also provides a model that can assist in controlling the calcination start location during operation to prevent the growth of mid-kiln rings.

Rotary lime kilns are used in the paper industry to convert lime mud to lime in the kraft recovery cycle. While lime kilns allow for long residence times to achieve good product quality, kiln operators still face problems in trying to obtain a uniform product [1]. One major issue that operators often face is ringing, where bed material sticks and accumulates to the surface of the kiln wall. While small rings are unavoidable during operation, these rings can grow and begin to impede bed and gas flow, impacting product quality. If a ring grows too large and does not break up during operation, the kiln must shut down to remove the ring [2].

Mid-kiln rings form near the middle of the kiln, which is near the start of the calcination reaction. These rings are the most common, and they are the most difficult to remove due to their location [2]. There are several possible mechanisms by which rings may form and deposit along the wall, including the following: melting of sodium compounds; agglomeration and sintering of particles; and recarbonation due to fluctuations in the start location of calcination [2]. When the calcination location shifts in the kiln, recarbonation can occur, potentially causing the bed material to harden onto the kiln wall. Constant fluctuations in kiln control can add new hardened layers to the ring over time, resulting in ring growth. While operators strive to maintain steady-state conditions within the kiln, changes in production are inevitable, and the harsh conditions within the kiln make it impossible to obtain direct temperature measurements. Control of the kiln is therefore dependent on inlet and outlet conditions, where the internal conditions are not known during operation. This motivates study of the transient behavior of lime kilns to better understand fluctuations of the bed temperature.

A detailed heat transfer model of a dry rotary lime kiln was developed, including modeling of the calcination reaction, to determine where calcination starts in the kiln, as well as the degree of calcination of the output lime. The objective of this work was to use this model to examine the impact of changing operating conditions on the calcination reaction. A sensitivity analysis was performed to determine which operating conditions have the largest impact on the calcination location and final calcination degree. The dynamic results of the model were compared to industrial data to validate the model. The change in calcination location was examined during a period of ringing in the kiln to examine the relationship between the two.

MATERIALS AND METHODS

The following sections briefly describe the model. More details are available in [3].

Gas model

A computational fluid dynamics (CFD) model in ANSYS Fluent (Ansys; Canonsburg, PA, USA) was developed to simulate the gas phase in a rotary kiln. The assumptions for the CFD gas model are listed here:

- Two-dimensional (2D) axisymmetric around the kiln centerline.
- Symmetric and concentric burner in the kiln.
- Gravity and buoyance effects are neglected.
- Physical bed is not present within the model.
- Pure methane fuel is used to simulate natural gas combustion.

A 2D axisymmetric model was chosen over a full three-dimensional (3D) model for reasons of computational efficiency, and also because Macphee [4] shows that temperature and heat flux predictions for a 2D and a 3D model are very similar. Since the gas model is axisymmetric, a physical bed is not present in the model; instead, mass and heat sinks are used to account for the thermal effects of the bed. While the industrial kiln being modeled uses natural gas as a fuel source, methane gas is modeled instead for simplicity. Radiation is modeled using the discrete ordinates (DO) model, where a weighted-sum-of-gray-gases model (WSGGM) is implemented to account for the radiation emitted by water (H_2O) and carbon dioxide (CO_2), rather than a simpler gray-gas approximation that would not be accurate for these real gases. The burner consists of a fuel inlet centered in the middle of the kiln, with the primary air inlet surrounding the fuel inlet; the secondary air inlet spans from the outer edge of the burner to the refractory wall. The secondary air temperature is estimated using an energy balance of the following: simulated outlet lime temperature; total mass of the secondary air entering the kiln; assumed final cooled temperature of 370°C; and assumed 80% efficiency in heat transfer from the outlet bed to the air.

Bed model

A one-dimensional (1D) bed model was used to simulate the mass and heat transfer occurring axially down the kiln. The assumptions for the 1D bed model are listed here:

- Bed is pure calcium carbonate.
- Particles are mono-sized and spherical.
- Calcination occurs as a shrinking core reaction.
- Bed is well-mixed and uniform in the transverse plane.

The bed material is assumed to be 100% calcium carbonate, where the bed particles are assumed to be mono-sized and spherical and calcination occurs as a shrinking core reaction [5]. The bed is assumed to be well-mixed in the transverse plane, where the bed properties and temperature vary only axially down the kiln. The mass balance of the bed at an axial position Z down the kiln is:

$$\dot{m}_{b,z+\Delta z} = \dot{m}_{b,z} - \dot{m}_{CO_2,z} \tag{1}$$

where:
$\dot{m}_{b,z+\Delta z}$ = mass flow of bed at axial position $z + \Delta z$, kg/s
$\dot{m}_{b,z}$ = mass flow of bed at axial position z, kg/s
$\dot{m}_{CO_2,z}$ = amount of CO_2 released at axial position z due to calcination, kg/s

The mass flow of the bed down the kiln is determined using Kramer's equation [6]. Kramer's equation has been extended to account for the transient effects of granular flow with changing operating conditions [7]. The kiln angle can be written in the form of an unsteady heat diffusion equation:

$$\rho c \frac{\partial \phi}{\partial t} = \frac{\partial}{\partial x}\left\{k \frac{\partial \phi}{\partial z}\right\} + S \tag{2}$$

The coefficients and source term, S, are nonlinear and given by:

$$\rho c = 2R^2 \sin^2 \phi \tag{3}$$

$$k = \frac{R^4 \sin^4 \phi}{C_A} \tag{4}$$

$$S = \left(\frac{3C_B R^3}{C_A}\right) \cos\phi \sin^2\phi \left(\frac{\partial \phi}{\partial z}\right) \tag{5}$$

where:
R = inner radius of the kiln, m
ϕ = half angle of the bed, rad
z = axial distance in the kiln, m
C_A = constant coefficient
C_B = constant coefficient

In Eq. 4 and Eq. 5, C_A and C_B are constants given as:

$$C_A = \frac{3 \tan\gamma}{4\pi n} \tag{6}$$

$$C_B = \frac{\tan\beta}{\tan\gamma} \tag{7}$$

where:
γ = static angle of repose of the bed, rad
β = inclination angle of the kiln from the horizontal, rad
n = rotation speed of the kiln, rev/s

Two steady-state boundary conditions are required to solve the unsteady bed height equation. The first boundary condition assumes that the bed height at the discharge end is equal to the discharge dam height. The second boundary condition is that the volumetric flow rate at the inlet is equal to the incoming load into the kiln. The initial condition is that the kiln load is assumed to be at steady-state, which is solved using Kramer's equation [6]. This allows the residence time of the bed to be modeled using the 1D bed equation.

Radiation to the bed is modeled using equations developed by Hottel and Sarofim [8]. Conduction and convection to the bed are modeled using equations developed by Tscheng and Watkinson [9]. Decomposition is simulated using a shrinking core model and is dependent on the difference in CO_2 concentration in the gas and the bed at the reaction front [10]. The gas and bed models are coupled via a volumetric mass source for CO_2 and a volumetric energy source. The energy equation for the bed includes the dynamic change in temperature, given as:

$$\frac{dE_{b,z}}{dt} + \dot{m}_{b,z} C_{p,b} \frac{dT_b}{dz} = \sum \dot{Q}_{g,w \to b,z} \tag{8}$$

where:
$E_{b,z}$ = energy in the bed at axial position z, J
t = time, s
$C_{p,b}$ = specific heat of the bed at axial position z, J/kg/K
T_b = bed temperature at axial position z, K
$\Sigma \dot{Q}_{g,w \to b,z}$ = sum of heat transfer rates from the gas and wall to the bed at axial position z, W

RESULTS AND DISCUSSION

The industrial kiln being modeled had a length of 85 m and an internal diameter of around 3.2 m. A variety of operating conditions are required as inputs into the model, such as: bed load entering the kiln, fuel flow rate, primary air flow rate, excess oxygen (O_2) at the gas outlet, kiln rotation speed, ambient temperature, mud solids, outlet gas temperature, and electrostatic precipitator gas temperature. The bed loading rate and kiln rotation speed are used to determine the mass flow rate of material down the kiln. The fuel flow rate and primary air flow rate are directly used in the gas model for combustion. The excess O_2 measurement at the gas outlet is used to estimate the amount of secondary air entering the kiln. The mud solids, gas outlet temperature, and electrostatic precipitator gas temperature are used to estimate the incoming feed temperature of the bed using an energy balance [3]. Finally, the ambient temperature is used to estimate the total heat loss in the kiln.

Steady-state results

Figure 1 shows the bed and average axial gas temperatures along the kiln. From left to right, the average gas temperature first rises and peaks due to combustion about 10 m from the tip of the burner in the kiln, then slowly decreases over the length of the kiln as heat is transferred to the bed and refractory wall. Going from right to left, the bed enters the kiln around 325°C, and the temperature increases almost linearly until around 57 m from the hot end. This is the start of calcination, where the bed slope changes rapidly due to heat now being absorbed by the reaction rather than increasing the temperature of the bed. The product bed temperature is around 1000°C, which agrees well with other model outputs of around 900°C–1100°C [11,12].

Figure 2 shows the measured (by thermal cameras) and simulated outer shell temperatures along the length of the kiln. There is some variability in the measured outer shell temperature, which is due to bearings and other components on the kiln, as well as being dependent on the refractory thickness at each location. In addition, the measured data is rough and the accuracy is difficult to deter-

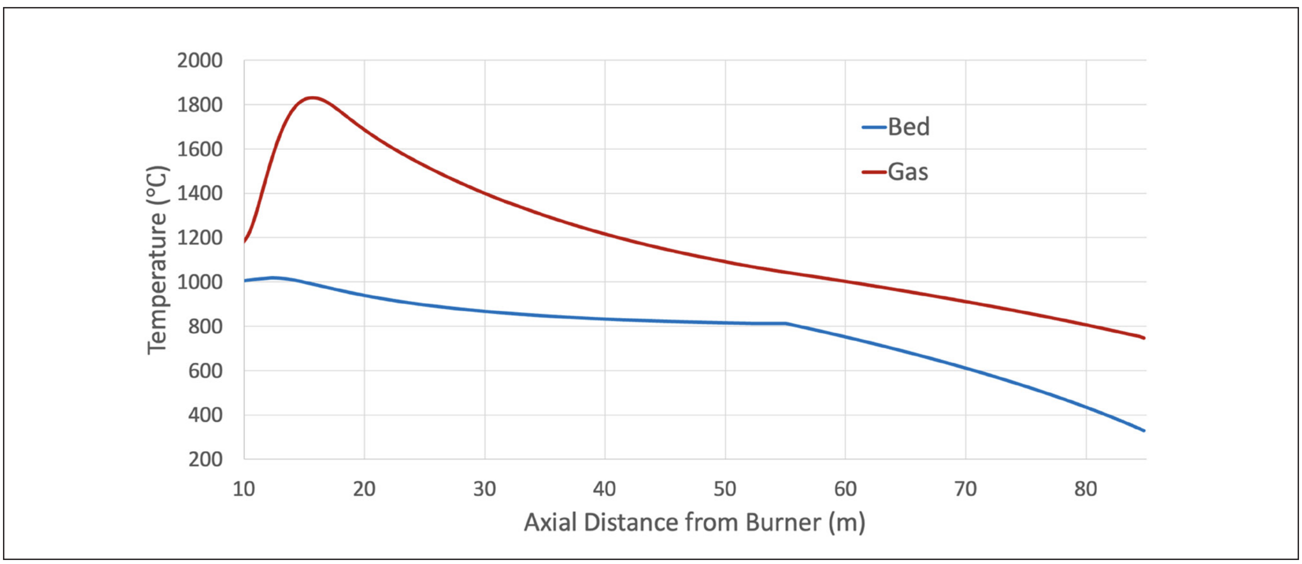

1. Simulated bed and average axial gas temperature down the kiln.

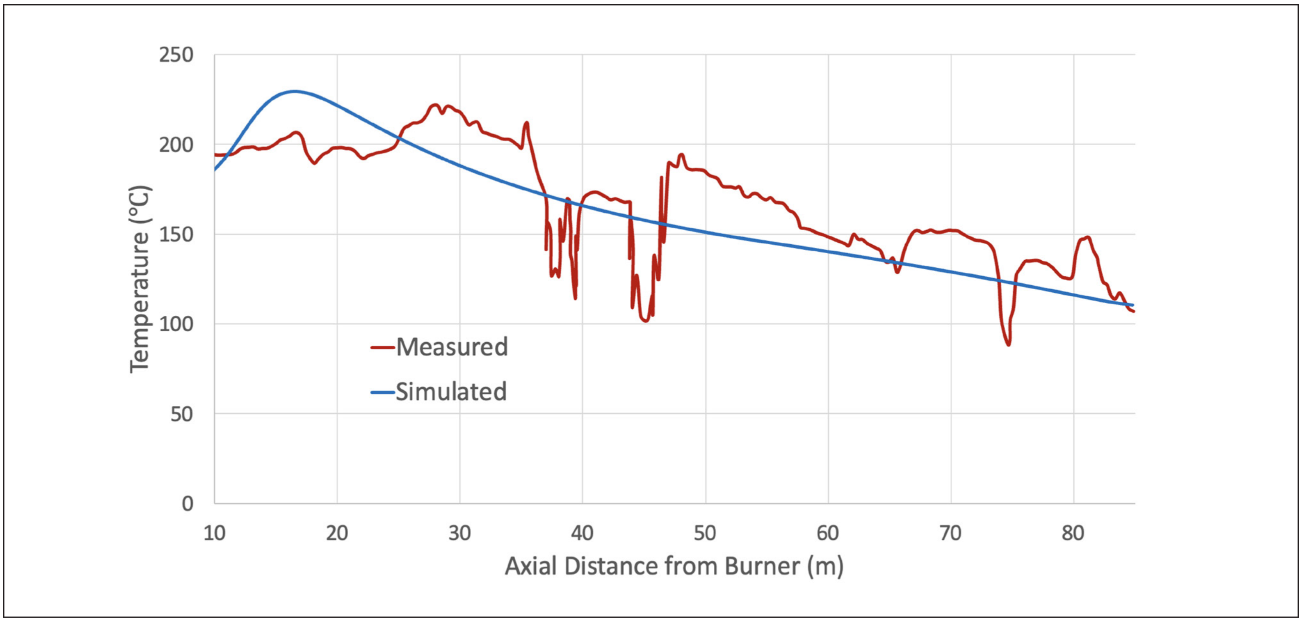

2. Simulated and measured outer shell temperature down the kiln.

mine. However, there still appears to be good agreement between the measured and simulated outer shell temperatures. Over the entire axial length of the kiln, the mean absolute error (MAE) between the measured and simulated outer shell temperature is 18.9°C. This helps to validate the heat loss calculation in the model.

Further analysis of the steady-state results can be found in our recent work [3]. This includes steady-state results as well as a sensitivity analysis for both a dry and wet kiln.

Sensitivity analysis

A sensitivity analysis was performed to determine which operating conditions and model parameters have the largest impact on the calcination location and calcination degree. A full detailed analysis of the sensitivity analysis results can be found in our recent work [3].

In summary, the two variables that have the largest impact on the calcination location are the fuel flow rate and the bed feed temperature. For regular loading, an increase/decrease in fuel flow rate by 10% moves the calcination start location 1.5 m towards the cold end and 1.8 m towards the hot end, respectively. Again, for regular loading, a decrease in the feed temperature by 50°C and 100°C both move the calcination zone by around 1.1 m toward the hot end. Similar trends can be seen for the low loading case as well. As mentioned earlier, the feed temperature is estimated based on an energy balance between the incoming load, the moisture content, and the change in gas temperature from the kiln outlet to the electrostatic precipitator. Therefore, the feed temperature is a large function of the moisture content, and it is clear that the fuel-to-load ratio and the moisture content have a large impact on the movement of the calcination location in the kiln.

Dynamic results

The PI system (Aveva; Cambridge, UK) data, which updates every 15 min from the industrial kiln, was used as input into the model for the dynamic simulations. This data included all the operating conditions required as input in order to run the model, as mentioned earlier. In July of 2021, the industrial kiln experienced a short period of accelerated ring growth, and this time period was therefore chosen as a period of interest for the dynamic modeling. Temperature measurements and predicted values were compared to determine model accuracy. The start of calcination was also examined to determine if a shift in the start location occurred during the ring growth in the kiln.

Figure 3 displays the measured loading and fuel flow rate to the kiln over a period of nine days. The kiln can be seen starting from low load after a shutdown in production, working back up to regular production during these nine days. After July 20, the kiln had reached regular operation and was back to operating roughly at steady-state. While this time period is of interest due to the ring growth, it also allows for determining the model accuracy for both regular loading and low loading operation.

Figure 4 displays the measured and simulated gas outlet temperature. At the start of the nine days, a sharp rise in outlet gas temperature corresponded to the kiln heating up after a full shutdown, and the fuel flow rate slowly increased over time. Overall, there was very good agreement between the measured and simulated data for the outlet gas temperature. The total average percent error during this time period for the simulated and measured outlet gas temperature was around 1.4%.

Figure 5 shows the measured and simulated outer shell temperature 45 m from the burner. The measured

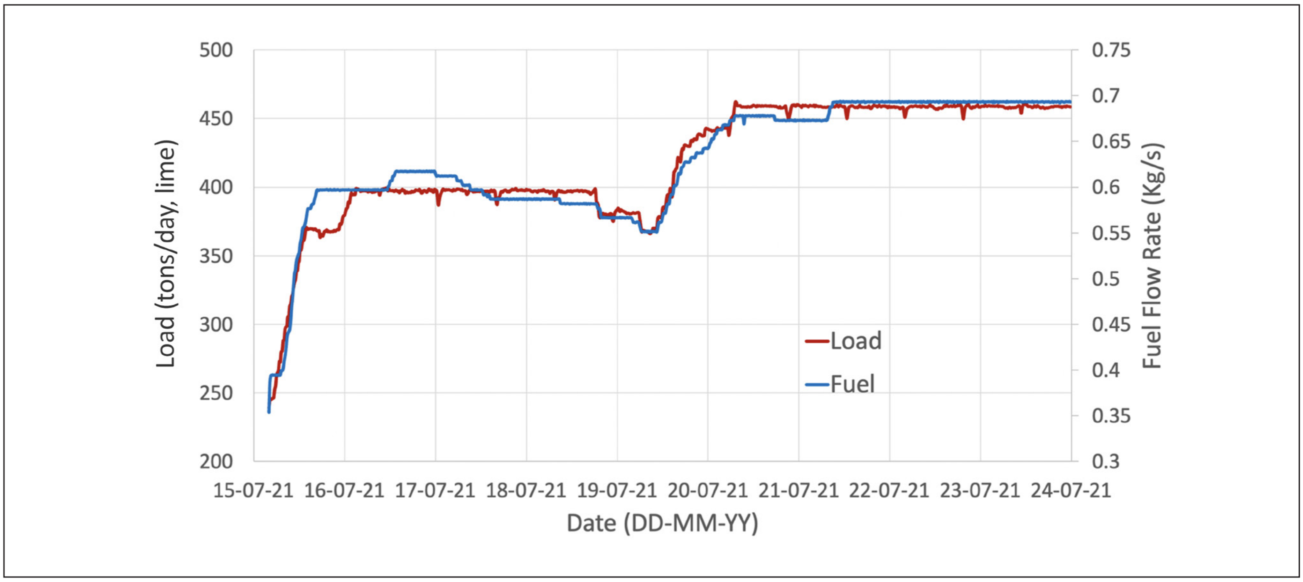

3. Load and fuel comparison over a 9-day period.

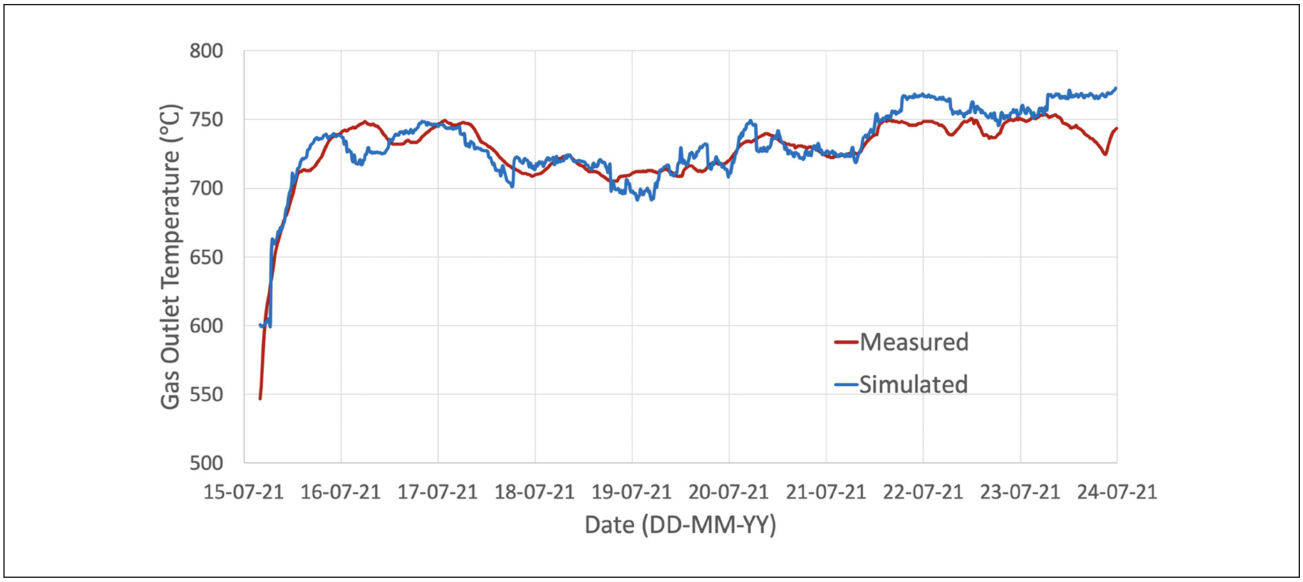

4. Measured and simulated center gas outlet temperature over a 9-day period.

value started colder than the simulated outer shell temperature because the industrial kiln was starting from shutdown, whereas the simulation assumes the kiln starts at steady-state and the refractory walls are already heated. After the kiln heated up, very good agreement was found between the measured and simulated data for the entire time period. The total average percent error during this time period for the simulated and measured outer shell temperature was around 2.7%, which helps to further verify the heat loss modeling.

Outer shell thermal images are used by the kiln operators to determine the degree of ringing in the kiln. **Figure 6** shows the outer shell temperature profile for the kiln when a ring was present on July 21 (top) and when the ring was broken up on July 22 (bottom), steadily increasing the rotation speed to increase the motion of the bed in an attempt to dislodge the ring before it hardened any further. The formation of the ring can be seen on the right of the kiln, where the outer shell temperature is cooler due to the insulation of the ring. The ring starts around 57 m from the hot end of the kiln and continues to the right.

From the results of the sensitivity analysis, the fuel flow rate and the feed temperature were the largest contributors to changes in calcination location. Therefore, these two variables were plotted against the predicted calcination start location in **Fig. 7** and **Fig. 8** to examine the correlation in more detail. From Fig. 7, during the initial start and heating of the kiln, there is a clear relationship between the calcination location and fuel/load ratio. However, afterwards, the fuel/load ratio became roughly constant,

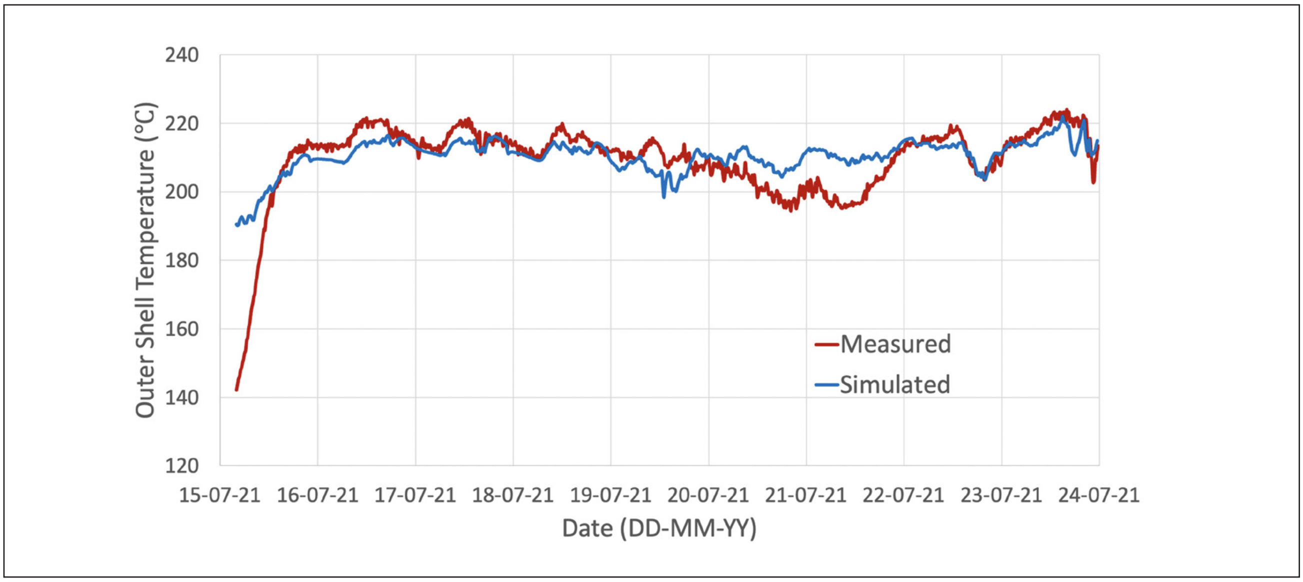

5. Measured and simulated outer shell temperature 45 m from the hot end over a 9-day period.

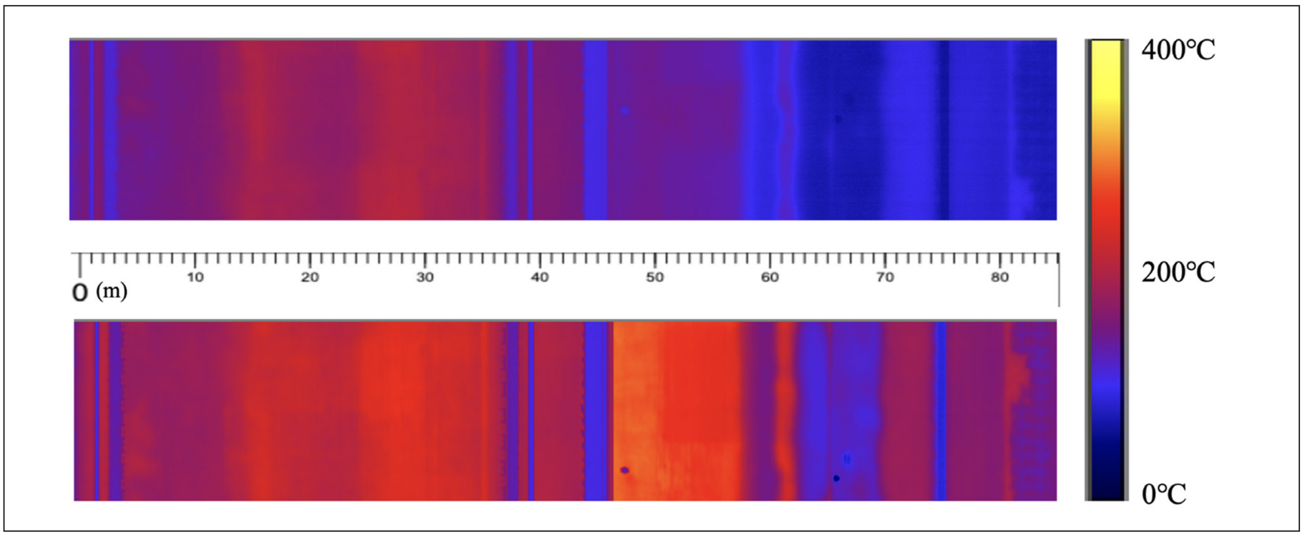

6. Thermal images of the outer shell temperature for the dry kiln with a ring growing (top), and with the ring broken up from an increase in rotation speed (bottom).

while the calcination location continued to fluctuate. These fluctuations in calcination location in the latter part of the time period can be explained by the feed temperature, as seen in Fig. 8. During the start of the time period, the feed temperature was mostly constant while the calcination start location fluctuated due to the fuel/load ratio. However, later on, the calculated feed temperature and calcination location were strongly correlated, while the fuel/load ratio was roughly constant. Since the feed temperature is a large function of the moisture content in the external dryer and cannot be controlled easily, control over the fuel flow rate to account for changes in feed temperature could keep the calcination location constant during operation to limit ring growth.

Comparing the dynamic change in the calcination location to the growth of the ring, a total shift of 4 m occurred over a 5-day period. During this time, the ring begins to grow rapidly, before being broken apart by the increase in kiln rotation speed. Therefore, it appears that the large shift in calcination location during this time period correlated with the increase in ring growth in the kiln. However, more data is required in order to have confidence in correlating the calcination start location to ring growth in the kiln.

CONCLUSIONS

A 2D axisymmetric CFD model with a 1D bed model was developed for a rotary lime kiln. The model can simulate both steady-state and transient conditions. The model was validated using temperature data from a mill, and good agreement was found for both the steady-state and transient

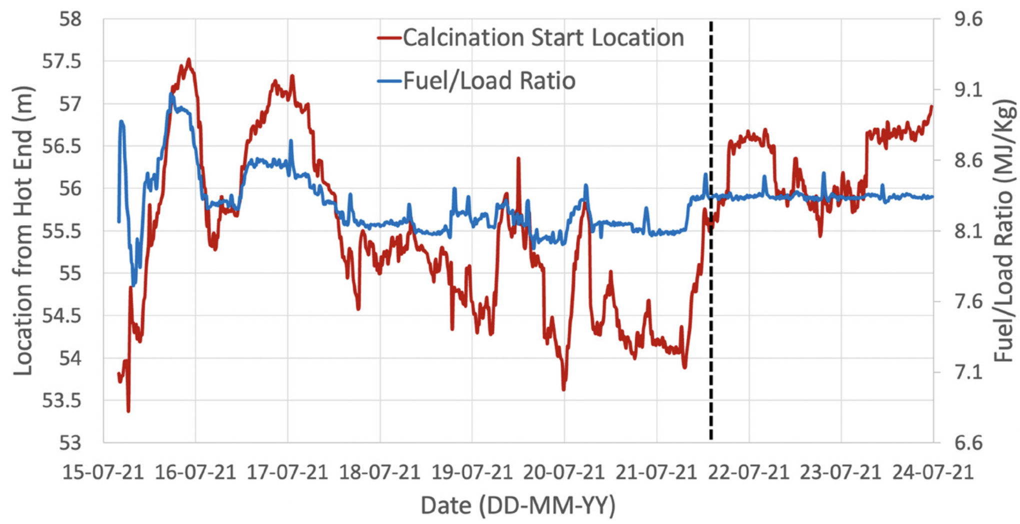

7. Calcination start location and the fuel/load ratio over the 9-day period, with a dotted line where the ring broke up due to an increase in rotation speed.

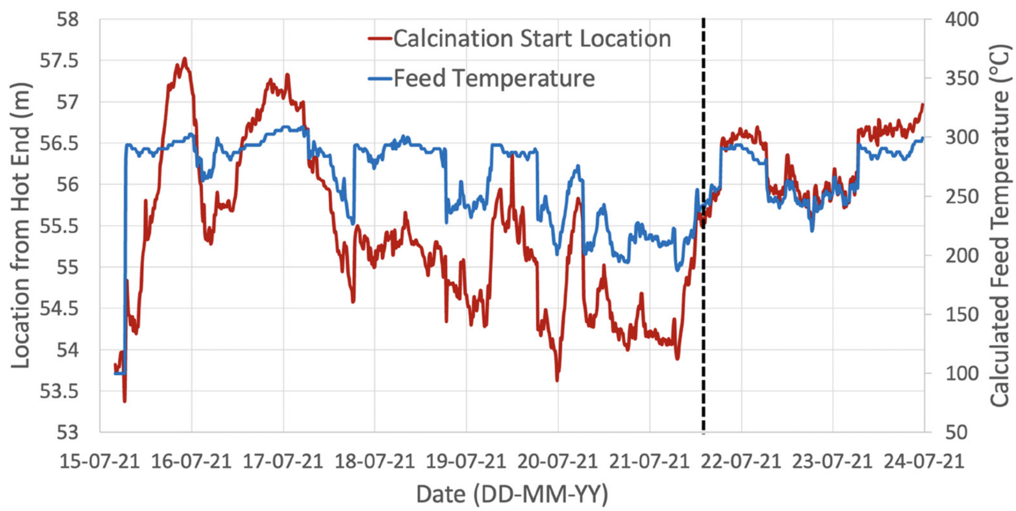

8. Calcination start location and estimated feed temperature over the 9-day period, with a dotted line where the ring broke up due to an increase in rotation speed.

simulations. The dynamic shift in calcination start location was investigated during a time of ring growth for the kiln. A total change of 4 m was observed in the calcination start location during the time of ring growth, indicating that variations in calcination location and ring growth may be correlated. However, more data and comparison are required to have confidence in correlating calcination location with ring growth.

Future work will involve modeling large amounts of transient data to generate more conclusive results. Thermal outer shell imaging will be used to identify ringing events and will be compared to large shifts in the calcination start location over time. The difference between the gas and the bed temperatures at the start of calcination will also be examined and compared to outer shell thermal imaging to determine the relationship between ringing and a low temperature difference at calcination. This will help to conclude whether shifts in the calcination location are a main factor in ring growth. Furthermore, future work is being done on modeling the bed in 3D to examine bed phenomena in more detail. Different operating conditions will be simulated to determine their effect on the change in velocity and temperature fields within the bed. This will give further insight into how heat transfer occurs within the bed and how this may impact calcination, ringing, and nodule formation. **TJ**

LITERATURE CITED

1. Boateng, A., "1 - The rotary kiln evolution and phenomenon," in *Rotary Kilns* (A.A. Boateng, Ed.), 2nd edn., Butterworth-Heinemann, Boston, 2016. https://doi.org/10.1016/B978-0-12-803780-5.00001-0.
2. Tran, H.N. and Barham, D., *Tappi J.* 74(1): 131(1991).
3. Ryan, J., Bussmann, M., and DeMartini, N., *Processes* 10(8): 1516(2022). https://doi.org/10.3390/pr10081516.
4. Macphee, J., "CFD modelling of a rotary lime kiln," MASc thesis, University of Canterbury, Christchurch, NZ, 2010.
5. Themelis, N.J., *Transport and Chemical Rate Phenomena*, Gordon and Breach, Basel, Switzerland, 1995.
6. Kramers, H. and Croockewit, P., *Chem. Eng. Sci.* 1(6): 259(1952). https://doi.org/10.1016/0009-2509(52)87019-8.
7. Spurling, R.J., Davidson, J.F., and Scott, D.M., *Chem. Eng. Res. Des.* 79(1): 51(2001). https://doi.org/10.1205/026387601528525.
8. Eckert, E.R.G., *AIChE J.* 15(5): 794(1969). https://doi.org/10.1002/aic.690150504.
9. Tscheng, S.H. and Watkinson, A.P., *Can. J. Chem. Eng.* 57(4): 433(1979). https://doi.org/10.1002/cjce.5450570405.
10. Bluhm-Drenhaus, T., Simsek, E., Wirtz, S., et al., *Chem. Eng. Sci.* 65(9): 2821(2010). https://doi.org/10.1016/j.ces.2010.01.015.
11. Agrawal, A. and Ghoshdastidar, P.S., *J. Therm. Sci. Eng. Appl.* 10(3): 031008(2018). https://doi.org/10.1115/1.4039299.
12. Georgallis, M., Nowak, P., Salcudean, M., et al., *Can. J. Chem. Eng.* 83(2): 212(2005). https://doi.org/10.1002/cjce.5450830208 .

ABOUT THIS PAPER

Cite this article as:
Ryan, J., Bussmann, M., and DeMartini, N., *TAPPI J.* 22(8): 520(2023). https://doi.org/10.32964/TJ22.8.520

DOI: https://doi.org/10.32964/TJ22.8.520

ISSN: 0734-1415

Publisher: TAPPI Press

About this journal

ABOUT THE AUTHORS

Ryan

Bussmann

DeMartini

My (Ryan's) Ph.D. research is focused on using CFD to simulate heat transfer within rotary lime kilns. A mill reached out with a ringing concern, and my research focus was then on modeling their kiln to determine if there is a way to mitigate ring growth during their operation.

Previous CFD models were often steady-state, whereas this research is transient and can model the changes in operating conditions over time. This model specifically looks at where calcination starts in the kiln and how that location changes over time, which is different from other CFD modeling for rotary kilns. Finally, this model is able to run in real time and could be used as a tool for kiln control.

The most difficult aspect of this research was modeling the movement of the bed over time, which has a large impact on heat transfer and calcination. Luckily, previous work has been done on modeling the height of the bed with changing loads and rotation speed, and this work was implemented into the model.

I personally discovered the difficulties in trying to use industrial data to model simulations. The accuracy of all the data can be difficult to determine, and small deviations in data can have a large impact on the results of the simulation.

The most surprising part of the research was how important the feed temperature is in where calcination first starts in the kiln. The fuel flow rate having a large impact on the calcination location is fairly obvious; however, the feed temperature, and therefore mud solids, have a much larger impact on calcination location than previously expected.

Mills can benefit from this information by measuring mud solids more frequently and ensuring this measurement is more accurate so they can adjust their fuel flow rate accordingly to account for changes in feed temperature. The model can also be used in real time to monitor the location of calcination, and it could be used to suggest the recommended fuel flow rate to keep the calcination location constant during operation.

The next steps will be working with the modeled mill to implement this model and determine how well the model can be used as a tool to control the calcination location during operation.

Ryan is a Ph.D. student and Bussmann is professor in the Department of Mechanical & Industrial Engineering, and DeMartini is professor in the Department of Chemical Engineering and Applied Chemistry, at the University of Toronto in Toronto, ON, Canada. Email Ryan at jarod.ryan@utoronto.ca.